(4)

CHEMICAL
RESEARCH,
DEVELOPMENT &
ENGINEERING
CENTER

CRDEC-TR-138

APPLICATION OF NOVEL DATA PROCESSING TECHNIQUES TO THE ANALYSIS OF ION MOBILITY SPECTROMETRY (IMS) DATA

Dennis M. Davis, Ph.D.
Robert T. Kroutil, Ph.D.

RESEARCH DIRECTORATE

January 1990

U.S. ARMY
ARMAMENT
MUNITIONS
CHEMICAL COMMAND

Aberdeen Proving Ground, Maryland 21010-5423

Disclaimer

The findings in this report are not to be construed as an official Department of the Army position unless so designated by other authorizing documents.

Distribution Statement

Approved for public release; distribution is unlimited.

UNCLASSIFIED

SECURITY CLASSIFICATION OF THIS PAGE

REPORT DOCUMENTATION PAGE

1a. REPORT SECURITY CLASSIFICATION UNCLASSIFIED	1b. RESTRICTIVE MARKINGS
2a. SECURITY CLASSIFICATION AUTHORITY	3. DISTRIBUTION/AVAILABILITY OF REPORT Approved for public release, distribution is unlimited
2b. DECLASSIFICATION/DOWNGRADING SCHEDULE	
4. PERFORMING ORGANIZATION REPORT NUMBER(S) CRDEC-TR-138	5. MONITORING ORGANIZATION REPORT NUMBER(S)
6a. NAME OF PERFORMING ORGANIZATION CRDEC 6b. OFFICE SYMBOL (if applicable) SMCCR-RSL	7a. NAME OF MONITORING ORGANIZATION
6c. ADDRESS (City, State, and ZIP Code) Aberdeen Proving Ground, MD 21010-5423	7b. ADDRESS (City, State, and ZIP Code)
8a. NAME OF FUNDING/SPONSORING ORGANIZATION CRDEC 8b. OFFICE SYMBOL (if applicable) SMCCR-RSL	9. PROCUREMENT INSTRUMENT IDENTIFICATION NUMBER
8c. ADDRESS (City, State, and ZIP Code) Aberdeen Proving Ground, MD 21010-5423	10. SOURCE OF FUNDING NUMBERS PROGRAM ELEMENT NO. / PROJECT NO. 1C162622 / TASK NO. A553C / WORK UNIT ACCESSION NO.

11. TITLE (Include Security Classification)

Application of Novel Data Processing Techniques to the Analysis of Ion Mobility Spectrometry (IMS) Data

12. PERSONAL AUTHORS (S)

Davis, Dennis M., Ph.D., and Kroutil, Robert T., Ph.D.

13a. TYPE OF REPORT	13b. TIME COVERED	14. DATE OF REPORT (Year, Month, Day)	15. PAGE COUNT
Technical	FROM 88 Feb TO 88 May	1990 January	27

16. SUPPLEMENTARY NOTATION

17. COSATI CODES			18. SUBJECT TERMS (Continue on reverse if necessary and identify by block number)
FIELD	GROUP	SUB-GROUP	IMS CAM Ion mobility spectrometry Data processing techniques Digital filtering
07	04		

19. ABSTRACT (Continue on reverse if necessary and identify by block number)

Over the past several years, novel data processing techniques have been developed for infrared spectroscopy. Many of these techniques use digital filters in the time domain to isolate spectral features. These techniques have use in other areas of spectral data processing. One of these areas is in the analysis of Ion Mobility Spectrometry (IMS) data. This work describes the preliminary investigation into this application.

(Keywords:)

20. DISTRIBUTION/AVAILABILITY OF ABSTRACT	21. ABSTRACT SECURITY CLASSIFICATION
[X] UNCLASSIFIED/UNLIMITED [ ] SAME AS RPT [ ] DTIC USERS	UNCLASSIFIED

22a. NAME OF RESPONSIBLE INDIVIDUAL	22b. TELEPHONE (Include Area Code)	22c. OFFICE SYMBOL
SANDRA J. JOHNSON	(301) 671-2914	SMCCR-SPS-I

DD FORM 1473, 84 MAR — 83 APR edition may be used until exhausted. All other editions are obsolete.

SECURITY CLASSIFICATION OF THIS PAGE

UNCLASSIFIED

PREFACE

The work described in this report was authorized under Project No. 1C162622A553C, Reconnaissance, Detection, and Identification. This work was started in February 1988 and completed in May 1988.

The use of trade names or manufacturers' names in this report does not constitute an official endorsement of any commercial products. This report may not be cited for purposes of advertisement.

This report has been approved for release to the public.

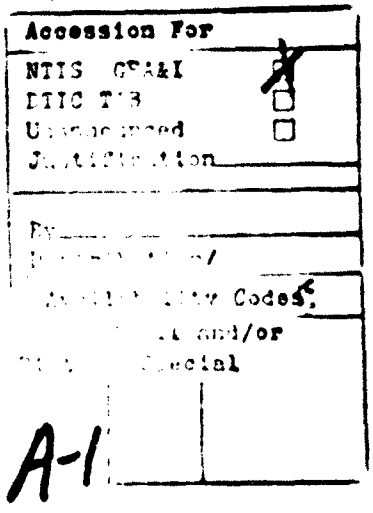

Blank

CONTENTS

LIST OF FIGURES

APPLICATION OF NOVEL DATA PROCESSING TECHNIQUES TO THE ANALYSIS OF ION MOBILITY SPECTROMETRY (IMS) DATA

1. INTRODUCTION

The data processing algorithm is one of the most important components in a detection system. Conventional data processing algorithms often rely on baseline correction techniques to correct for baseline slope before peak picking routines are used. One problem resulting from this baseline correction is the risk of being unable to identify a peak that is either present as a shoulder on another peak or located adjacent to one with much greater magnitude. In the case of chemical agent detectors, it is essential that this type of false negative be avoided. Therefore, an effort has been made to apply novel signal processing techniques to analyze the Ion Mobility Spectrometry (IMS) spectral signatures to eliminate the baseline correction procedure. Actual IMS signatures generated in tests of the Chemical Agent Monitor (CAM) were used as a data set. This effort was made to determine if several signal processing techniques developed for the XM21 remote chemical sensor[1] could be used for the discrimination of IMS or CAM data. This report describes the results of preliminary experiments and is divided into three major areas:

- Transfer of data
- Generation of a database
- Application of novel signal processing techniques

2. DATA MANIPULATION

2.1 Data Transfer.

The first major effort was the creation of two data transfer routines. The first data transfer routine was written on an International Business Machines personal computer (IBM-PC) to transfer an entire disk of binary data files collected from a Nicolet 4094A oscilloscope. The data transfer routine between the Nicolet oscilloscope and the IBM-PC was written in a compiled BASIC language.[2] The BASIC language program can read the file from the Nicolet oscilloscope storage device and also store the sequential file of intensity versus relative CAM drift time

---

[1]Small, G.W., Kroutil, R.T., Ditillo, J.T., and Loerop, W.R., "Detection of Atmospheric Pollutants by Direct Analysis of Passive Fourier Transform Infrared Interferograms," Anal. Chem. Vol. 60, pp 264-269 (1988).

[2]Davis, D.M., and Emory, S., IMSPEC, unpublished data, 1988.

on the IBM-PC hard disk drive. The data on the IBM-PC was stored in an 8-bit American Standard Code for Information Interchange (ASCII) format. The second step of the data transfer process was to transfer the IBM-PC ASCII files to a Honeywell Level 6 minicomputer. This transfer is accomplished through the file transfer routines that are contained in a commercial software package. The commercial software package transferred the ASCII data in serial format at 9600 baud using the protocol KERMIT.

2.2 Database Generation.

The second major effort was the generation of an IMS database on the Honeywell Level 6. The database was designed to eventually include all IMS data collected from a variety of sources. Presently, the database includes only a limited number of CAM or IMS spectra that were transferred as a result of this effort (159 spectra). The 159 CAM spectra were created by defining header information for each spectrum to be included in the database. The header information for each file includes the following:

- FILENAME. A description of the file contents.
- RUN NUMBER. Nicolet Disk ID Code.
- AGENT CONCENTRATION. Concentration of the chemical agent.
- INTERFERANT CONCENTRATION. Concentration of the interferant in the study or the concentration of the simulant or compound studied.
- TEMPERATURE. Temperature in the room on the day the spectrum is recorded.
- RELATIVE HUMIDITY. Relative humidity in the room on the day the spectrum is recorded.
- BAR RESPONSE. CAM response to the vapor challenge.
- MODE. Whether trying to detect nerve agents and positive ions (G Mode) or blister agents and negative ions (H Mode).
- INSTRUMENT SERIAL NUMBER. CAM serial number or other instrument identifier
- OPERATOR. Person who is responsible for recording the spectrum.
- COMMENTS. Any comments the operator deems important about the spectrum.

The header information for the database is stored as free format with a data key at the start of the header information to indicate the number of header fields and their data length. If required, additional header information can be added to the database.

The second step in generating the database is the data reduction process. Data that has been collected on the Nicolet oscilloscope normally has 3968 data points. The data reduction involves decreasing the number of data points in the spectrum from 3968 to 512. The final number of data points is still twice as many data points as used by the CAM algorithm. This increase in the number of data points over that used in CAM gives greater resolution in the processed spectra; no new information can be gained by the increased resolution of the data file. The number of data points was selected as a power of two so that many of the XM21 computer programs [e.g., Fast Fourier Transforms (FFT), Maximum Entropy Methods (MEM), etc.] could be used on the CAM data. In addition to the deresolution of the Nicolet data, the spectrum was converted by normalizing with respect to the X-axis. To do this, each value on the X-axis was divided by the value position of the reactant ion peak. For negative mode spectra, the peak position with the maximum intensity between 6.0 and 7.0 ms was used for the identification of the reactant ion peak. For positive mode data, a value between 6.5 and 7.5 ms drift time was used as a window in which to find the reactant ion peak. This resultant spectrum appears as a pseudo-frequency domain spectrum to the XM21 software. This new spectrum also appears to be a pseudo-reduced mobility spectrum that has a dimensionless X-axis corresponding to a ratio of drift times. Only the data in the range 0.5-3.0 along the ratio of drift time axis are stored. The resolution of the X-axis in the stored data files had a relative ratio of drift time equal to 0.05. This finalized version of the spectrum, along with the header information, is stored in the database for future use. A table of contents of the database is included in the Appendix.

2.3 Development of Digital Filters.

The third effort in this process is applying novel processing techniques to the CAM data in an attempt to eliminate background features. For this work, we decided to limit the processing techniques to those that were not computer intensive (i.e., those that do not require a large amount of computer processing time). Curve fitting, spectral deconvolution, and digital filtering are among the techniques that fit this criterion. The application of curve fitting routines involves fitting a polynomial expression to the background spectral features and subtracting this expression from the overall spectrum. Typically, this procedure does not work very well because the background features are difficult to fit with a polynomial expression. In addition, in the case of IMS spectra, the spectral features can change as a result of changing the concentration of the challenge. A better approach is the

technique of spectral deconvolution. In spectral deconvolution, an inverse Fourier transform would be applied to a raw IMS spectrum, to create the time-domain spectrum. Subsequently, apodization functions that use the spectral resolution features to select the bands of interest are applied to the spectrum. Another technique similar to spectral deconvolution is digital filtering. Digital filtering has two advantages over spectral deconvolution in that digital filters may be applied to either time- or frequency-domain spectra, and the spectral cutoff frequencies can be optimized for a given set of conditions. Like spectral deconvolution, the digital filters to be applied in the time domain can be inverse Fourier transformed and applied to the raw spectrum. For this work, digital filtering in the time domain was chosen as the signal processing technique because the routines for applying digital filters already exists within the XM21 software.

Time-domain digital filters are data transforms that operate on time-domain signals in a manner that is dependent on the frequency of the signal. These filters represent standard techniques in signal processing.[3] The simplest form of digital filter, termed a nonrecursive filter, has the form

$$Y^*_i = f_1 Y_{i-n} + \ldots + f_{n+1} Y_i + \ldots + f_{2n+1} Y_{i+n} \qquad (1)$$

where each filtered data point, Y^*_i, is defined as a sum of $2n + 1$ terms based on the corresponding raw data point, Y_i, and the raw data points surrounding Y_i. Each term is weighed by a different coefficient, f_i through f_{2n+1}.

In an interferogram, the raw data are actually a sum of frequencies. The filter acts by suppressing the amplitude of certain frequencies while amplifying others. The values of the coefficients determine the frequency dependence of the digital filter. The procedure for deriving the digital filter must be general and amenable to modification for different target chemical species with correspondingly different characteristic frequencies.

Because XM21 based interferogram software is being used, the derivation of the filter coefficients must begin in the frequency domain. Effectively, a frequency filter is desired that possesses a band-pass centered on a characteristic spectral feature of the target species. The interferogram filter will operate on the interferogram points in the same manner as the

---

[3]Childers, D., and Durling, A., Digital Filtering and Signal Processing, West Publications., St. Paul, MN, 1975.

frequency domain filter operates on the frequency data points. In Fourier terms, the multiplication of the raw spectrum and the filter spectrum in the frequency domain represents a convolution. The analogous action in the time domain involves evaluating the convolution integral of the corresponding time-domain functions. The derived digital filter allows this convolution integral to be approximated. The derivation of the digital filter can be reduced to a search for the set of coefficients that relate the raw and filtered interferograms. Once derived, these coefficients should be applicable to any other interferogram, or rather any CAM frequency-domain spectrum.

An inspection of equation 1 reveals that the nonrecursive filter is merely a linear model that relates a dependent variable, Y^*, to a set of independent variables, Y. The dependent variable is simply the filtered interferogram obtained through the action of the desired frequency filter and subsequent inverse Fourier transformation. The independent variables are defined by the raw unfiltered interferogram points. The computation of the best filter coefficients can be considered a problem in multiple linear regression analysis. The regression analysis was performed using the raw interferogram as the independent variable.

In any multiple regression analysis, the selection of independent variables is an important task. In the current problem, this equates with which data points around the point being filtered will be used in the filtering process. In regression analysis, there are a number of techniques available to aid in this selection (e.g., stepwise regression and best subset regression). For this study, the filter was constructed with consecutive points behind the filtered point. This derived digital filter of points behind the filtered point was used because preliminary results from the XM21 data indicate a filter with a higher R-squared (i.e., a higher correlation coefficient) value can be obtained. Further work on the CAM data needs to focus on the number of points used, the position of the points used, and the type of frequency-domain filtering function. When the filter was derived for the CAM data, consecutive terms were added to the filter until the correlation coefficient in the regression stabilized.

Using digital filtering points behind the point to be filtered yields a modified equation 2 where

$$Y^*_i = f_i Y_{i-n} + \ldots + f_{n+1} Y_i \qquad (2)$$

The optimum filter included 15 terms consisting of the raw data point and the 14 previous data points. The correlation

coefficient for the regression was 0.975; whereas, the F value for the significance of the regression was 2.05.

3. RESULTS AND DISCUSSIONS

Before any advanced data processing was performed, it was important to know what information was available in the original spectra. Four spectra that are contained in the database are shown in Figure 1. The spectra labeled 93 and 94 are the modified CAM spectra (i.e., those modified for the database as described above) that are obtained when the CAM is exposed to a vapor challenge containing 0.1 µg/L of phenol in air. The CAM exhibited no bar response to the vapor challenge of the phenol at this concentration. Spectra 108 and 109 are the modified CAM spectra that are obtained when the CAM is exposed to a vapor challenge containing 0.1 µg/L of phenol and 0.16 µg/L of mustard (HD) (bis-dichloroethyl sulfide) in air. The CAM exhibited a 3-bar response to spectrum 108 and a 2-bar response to spectrum 109. As an aid in viewing the spectral detail, an enlargement of the 1.1-1.8 ratio-of-drift-time region of Figure 1 is shown in Figure 2.

To determine the effects of higher concentrations of phenol and/or HD on the spectral features obtained on the CAM, a number of other spectra were obtained. The next four spectra used in this study are shown in Figures 3 and 4. Figure 3 shows the modified CAM spectra contained in database files 118, 119, 131, and 133. Spectra 118 and 119 are the spectra that are obtained when the CAM is exposed to a vapor challenge containing 0.3 µg/L of phenol and 0.16 µg/L of HD. The CAM did not exhibit any bar responses to the vapor challenges; an example of a false negative situation. Spectrum 131 is the modified CAM spectrum that was obtained when the CAM was exposed to a vapor challenge containing 1.0 µg/L of phenol and 0.16 µg/L of HD. Again, the CAM exhibited no bar response to the vapor challenge. The last spectrum shown in Figures 3 and 4 is spectrum 133. This modified CAM spectrum was obtained when the CAM was exposed to a vapor challenge containing 1.0 µg/L of phenol and 0.4 µg/L of HD. The CAM had a 4-bar response to the vapor challenge used for spectrum 133. Figure 4 is an enlargement of the 1.1-1.8 ratio-of-drift-time region of Figure 3.

An Inverse Fast Fourier Transform (IFFT) has been applied to each spectrum described above, resulting in a time domain spectrum much like one would deal with in infrared spectroscopy. This procedure is performed because the software used in this study has been adapted from infrared spectroscopic studies. Subsequently, an FFT is applied to each spectrum to recreate the initial frequency-domain spectrum. These two manipulations of the original data were performed to aid in the visualization of whether any improvements can be made as a result of a linear digital filter.

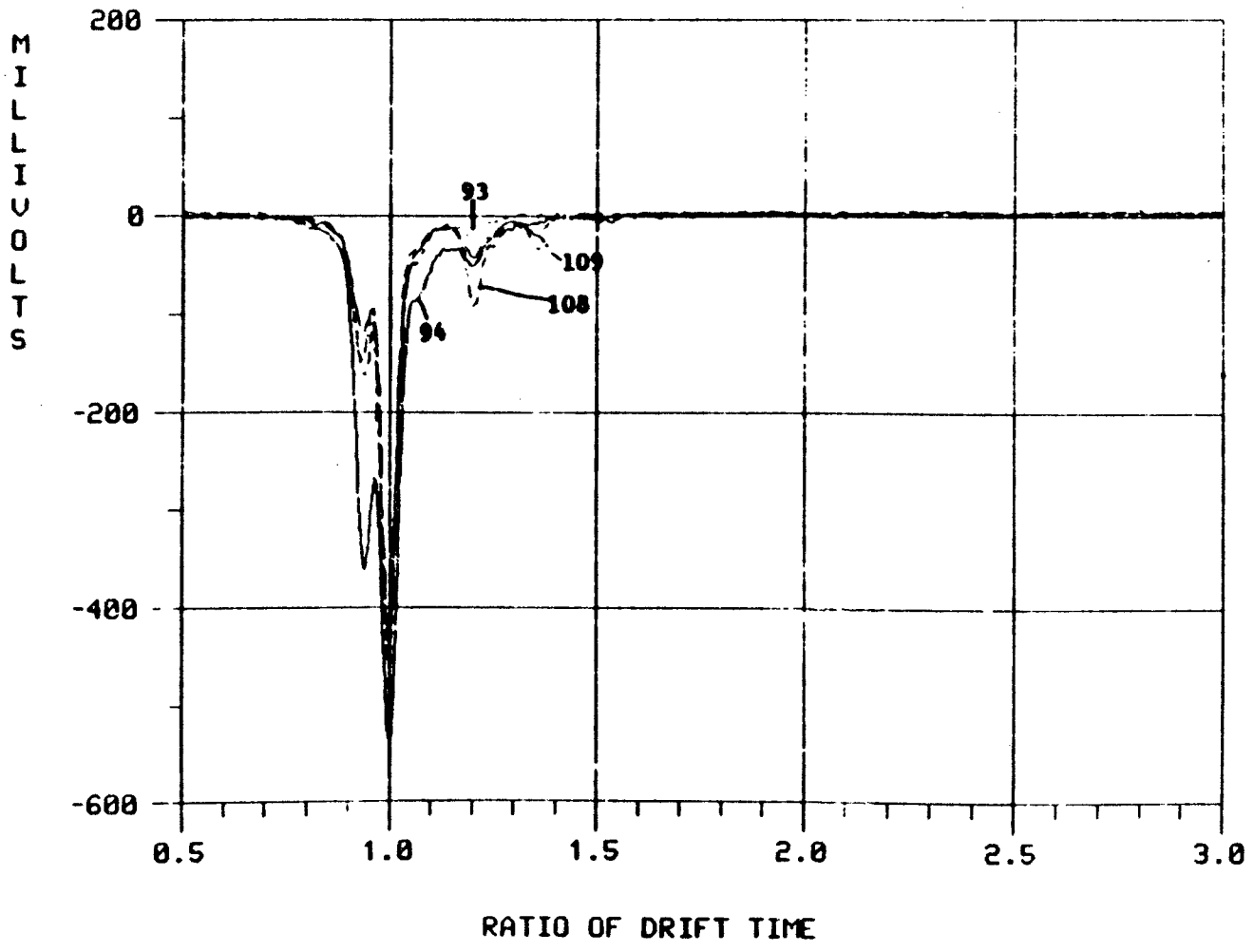

Figure 1. IMS Spectra of Phenol and HD from 0.5 to 3.0 Ratio of Drift Times. The concentration of phenol is 0.1 µg/L of air for all spectra; the concentration of HD is 0.16 µg/L of air for spectra 108 and 109. No HD is present for spectra 93 and 94.

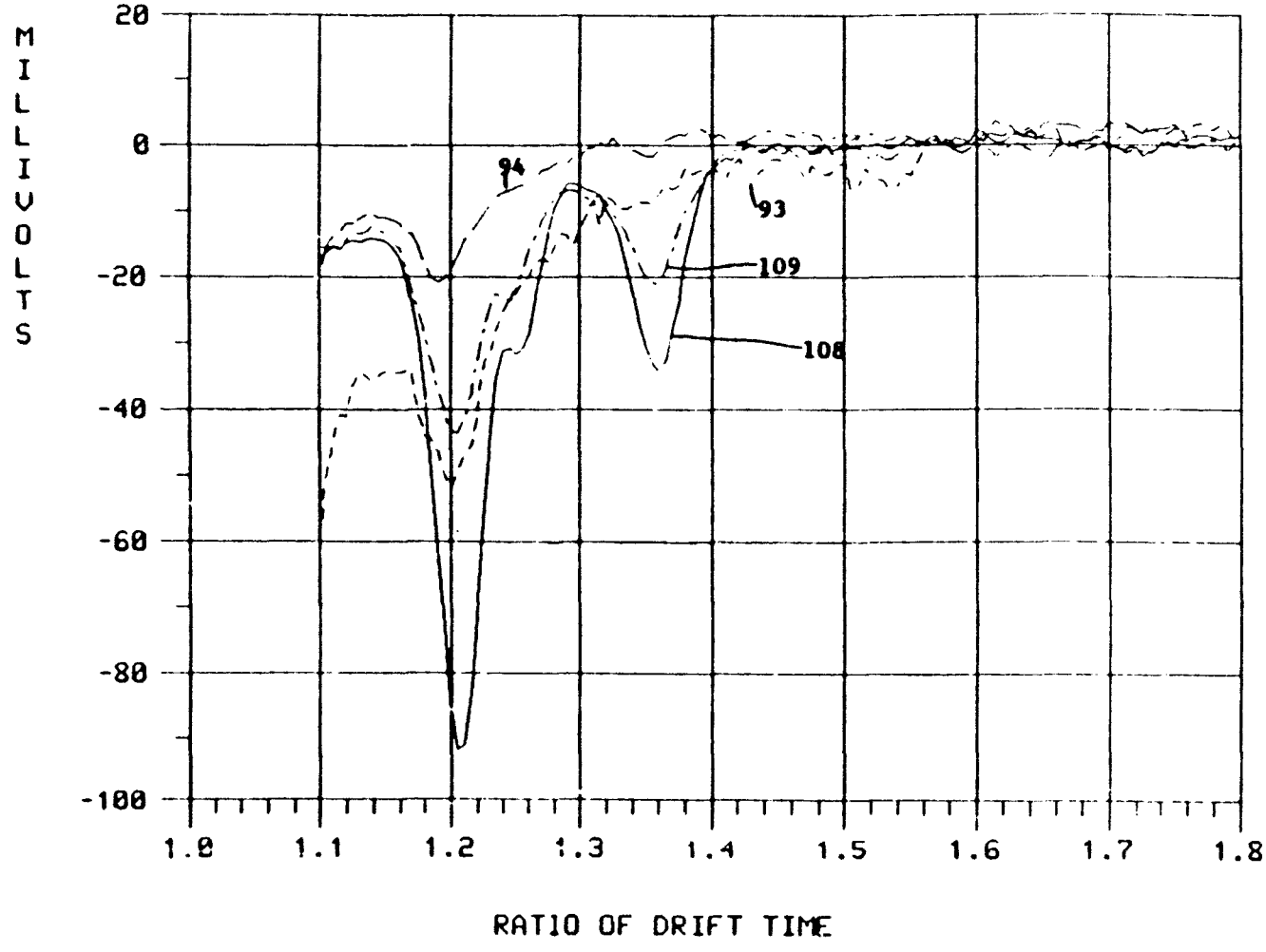

Figure 2. IMS Spectra of Phenol and HD from 1.1 to 1.8 Ratio of Drift Times. The concentration of phenol is 0.1 µg/L of air for all spectra; the concentration of HD is 0.16 µg/L of air for spectra 108 and 109. No HD is present for spectra 93 and 94.

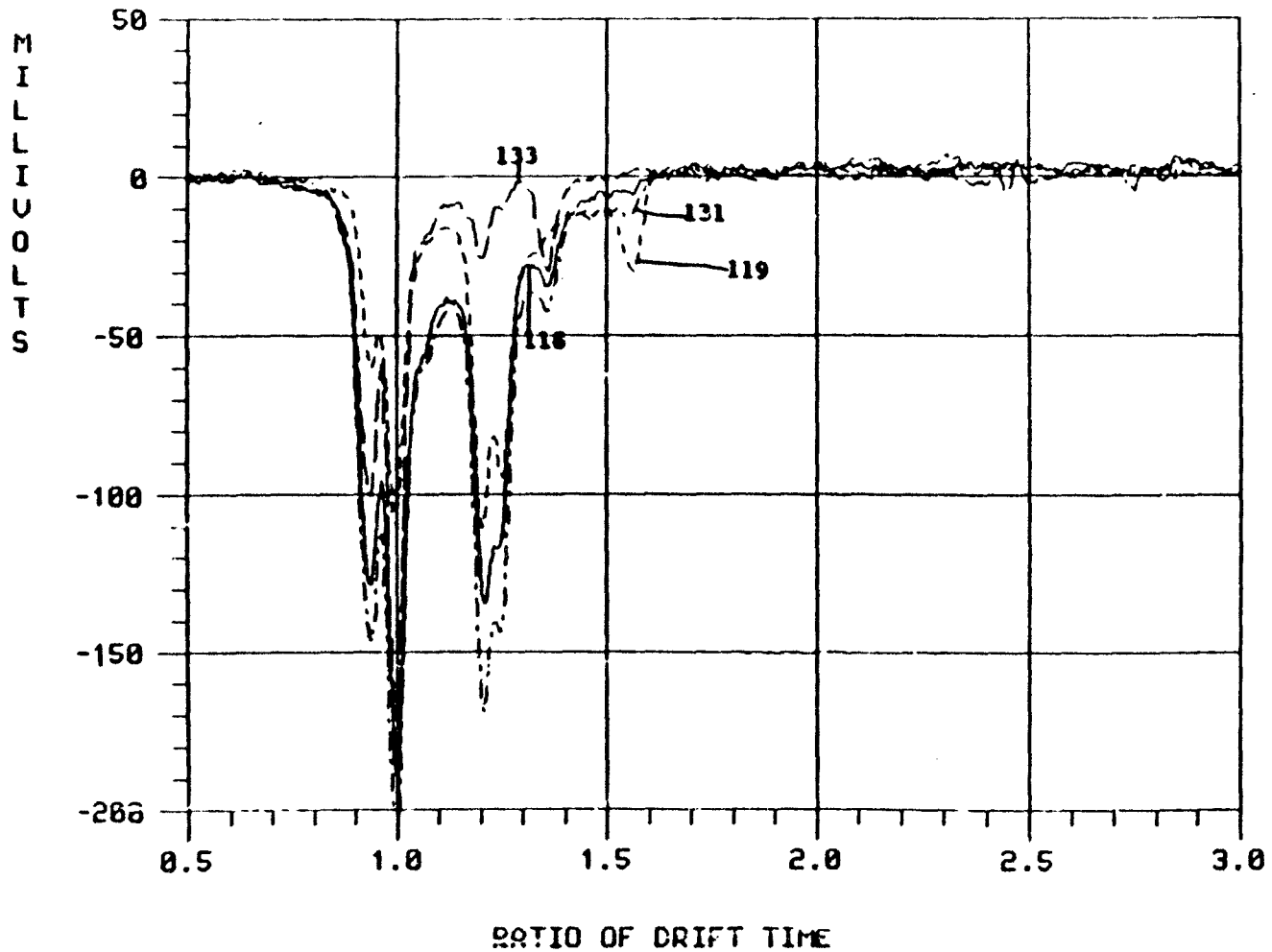

Figure 3. IMS Spectra of Phenol and HD from 0.5 to 3.0 Ratio of Drift Times. The concentration of HD is 0.16 µg/L of air for spectra 118, 119, and 131, and 0.4 µg/L of air for spectrum 133; the concentration of phenol is 0.3 µg/L of air for spectra 118 and 119 and 1.0 µg/L of air for spectra 131 and 133.

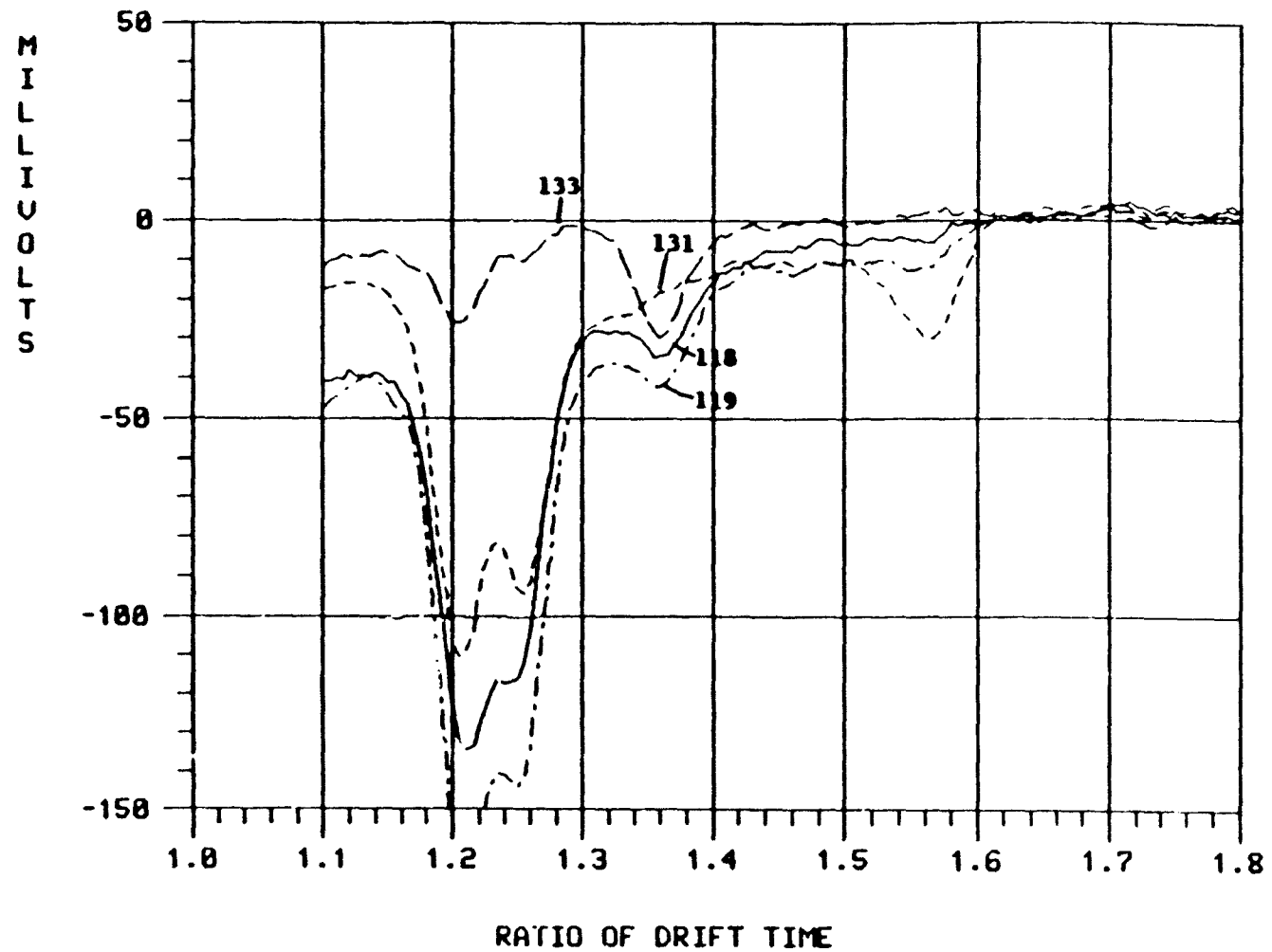

Figure 4. IMS Spectra of Phenol and HD from 1.1 to 1.8 Ratio of Drift Times. The concentration of HD is 0.16 µg/L of air for spectra 118, 119, and 131, and 0.4 µg/L of air for spectrum 133; the concentration of phenol is 0.3 µg/L of air for spectra 118 and 119 and 1.0 µg/L of air for spectra 131 and 133.

The resultant spectra are shown in a stacked spectrum plot in Figure 5. Each spectrum in the plot has been scaled so that the maximum peak height of any one spectrum is the same as the maximum peak height of all the other spectra. These peak intensities have not been changed, only the plot size. The dashed line in Figures 5 through 8 is located at a ratio-of-drift-time value of 1.39. This is the value at which one would expect to find the HD ion peak. An enlargement of the 1.1-1.8 ratio-of-drift-time region of Figure 5 is shown in Figure 6.

An IFFT has been applied to each spectrum contained in the database to create a time-domain spectrum. A digital filter, corresponding to a Gaussian-shaped peak that is four data points wide and centered at 1.39 on the ratio-of-drift-time axis, was applied to the time-domain spectrum. After the digital filter, an FFT was performed to give a modified IMS spectrum. A stacked plot of all eight spectra, after application of the digital filter, is shown in Figures 7 and 8. Again, each spectrum in the plot has been graphically scaled so that the height of the most intense peak in any one spectrum is the height of the most intense peak in all of the other spectra in the plot. An enlargement of the 1.1-1.8 ratio-of-drift-time region of Figure 7 is shown in Figure 8.

A comparison of Figures 5 and 7 shows the enhancement that has been gained as a result of the digital filter. In Figure 7, spectra 108, 109, and 133 have, as the major spectral feature, a peak at a ratio of drift time of 1.39. The corresponding spectra in Figure 5 exhibit only minor spectral features at this value of the ratio of drift time. Spectra 118 and 119 in Figure 7 have a peak at a ratio of drift time of 1.39 as one of the two major spectral features; whereas, the corresponding spectra in Figure 5 exhibit only minor spectral features. Spectrum 131 in Figure 7 exhibits what may be a peak at the ratio-of-drift-time value of 1.39; however, at this time, identification of this feature as the HD peak would be difficult. Spectrum 131 in Figure 5 shows no spectral feature at the proper location; therefore, it is impossible to identify the presence of HD. The last spectra shown in Figures 5 and 7, spectra 93 and 94, are noisy after application of the digital filter, as shown in Figure 7. This is because no peak is present in the original spectra at the location of the digital filter.

4. CONCLUSIONS

Significant improvement has been shown as a result of applying a simple digital filter to CAM data. It has been demonstrated that in cases in which materials of interest (e.g., HD) are mixed with interferants (e.g., phenol) and the ratio of the HD concentration to phenol concentration ranges from 2:1 to 1:2.5, one can clearly resolve the presence of and identify

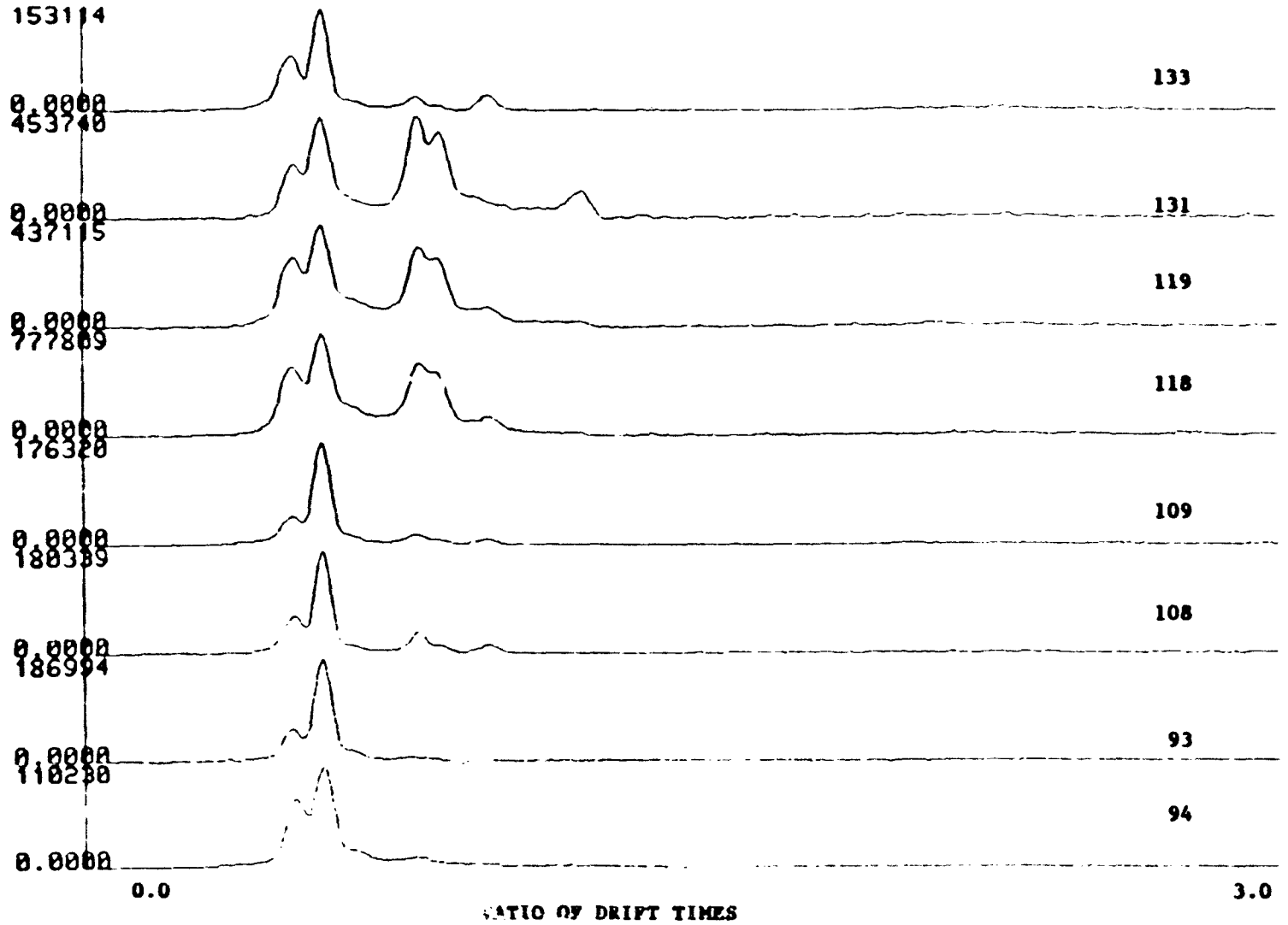

Figure 5. IMS Spectra of Phenol and HD After Application of an IFFT and an FFT. Spectral range for the X-axis is 0.0-3.0 ratio of drift times, and the Y-axis units are arbitrary.

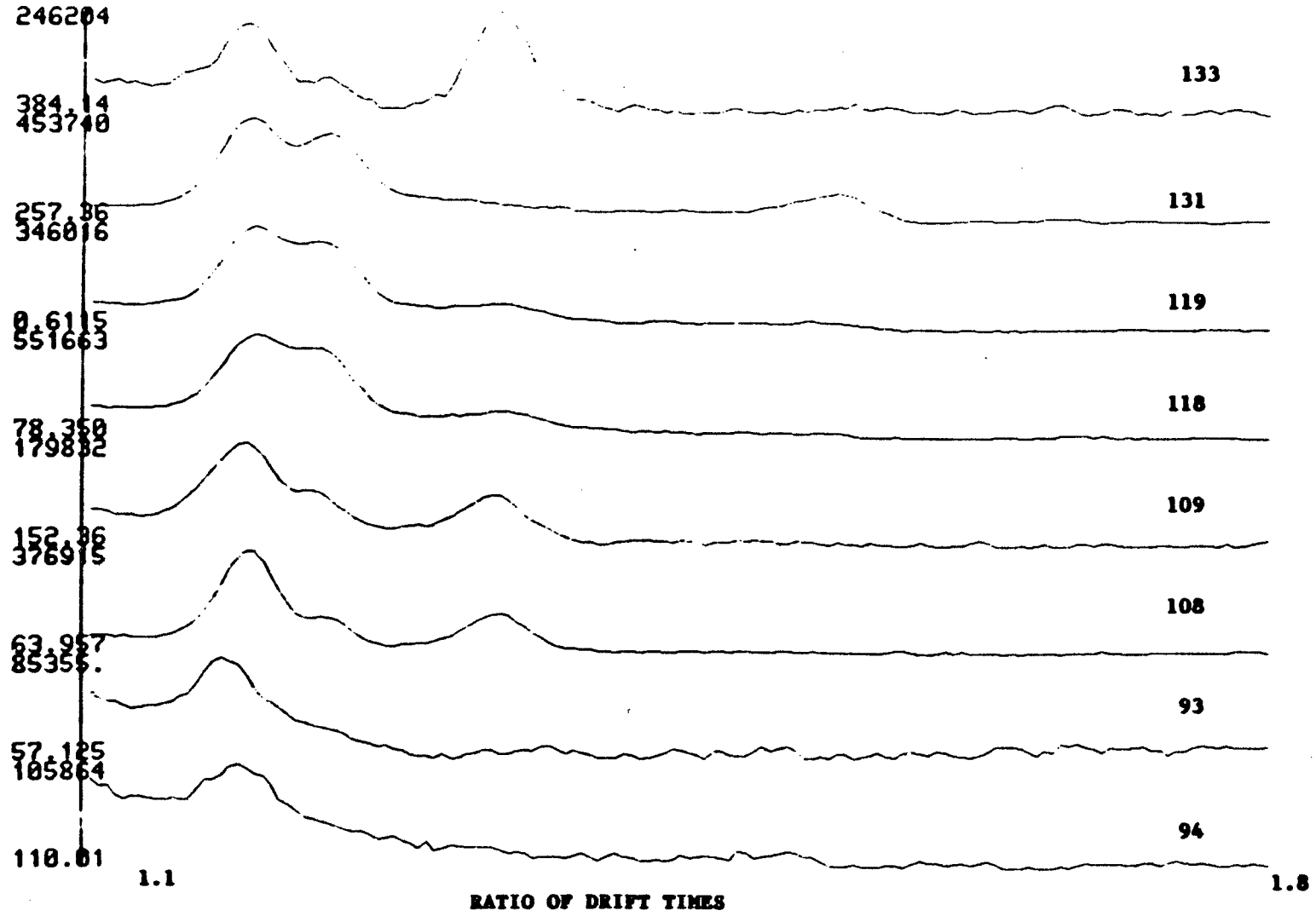

Figure 6. IMS Spectra of Phenol and HD After Application of an IFFT and an FFT. Spectral range for the X-axis is 1.1-1.8 ratio of drift times, and the Y-axis units are arbitrary.

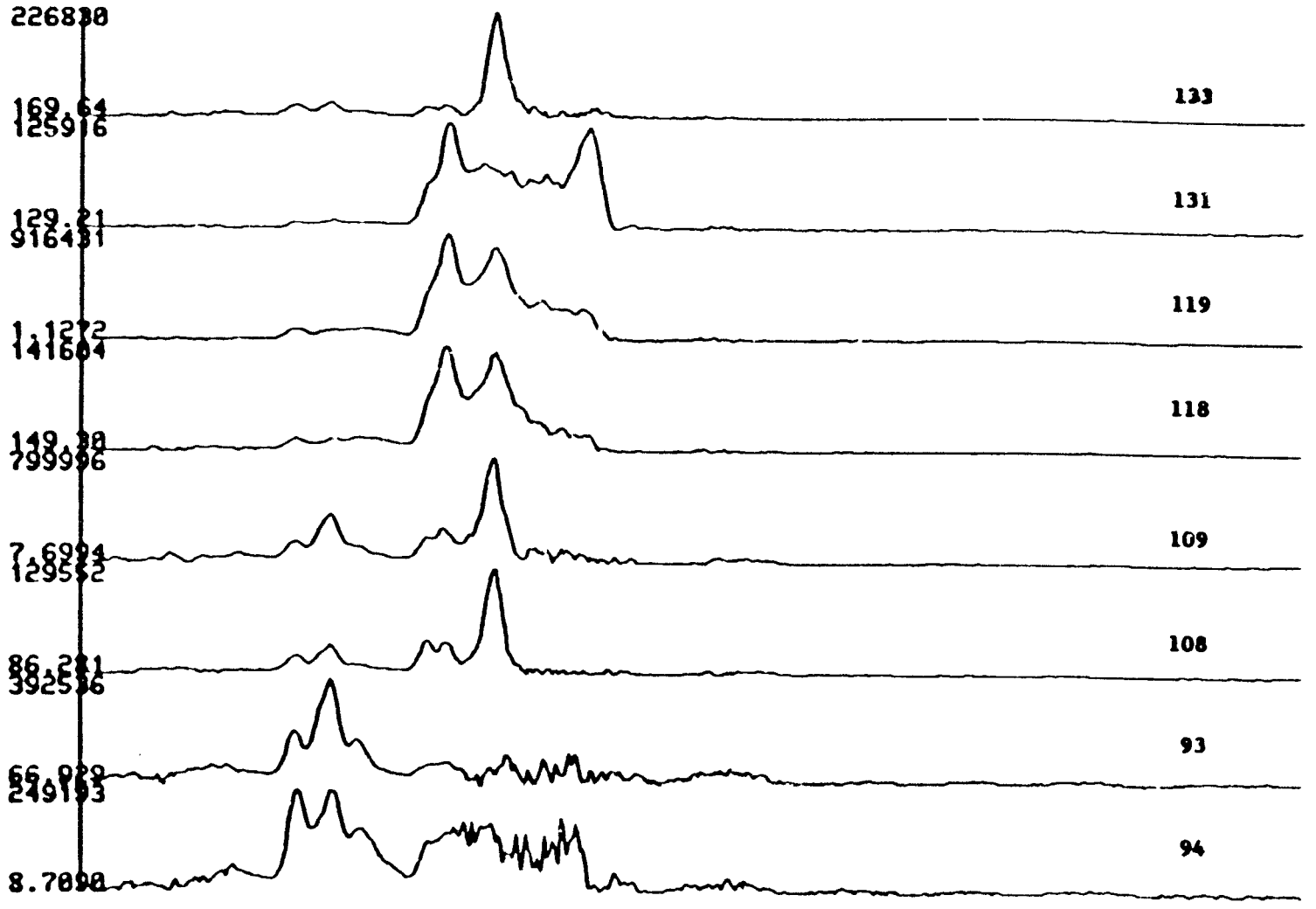

Figure 7. IMS Spectra of Phenol and HD After Application of an IFFT, the Digital Filter, and an FFT. Spectral range for the X-axis is 0.0-3.0 ratio of drift times, and the Y-axis units are arbitrary.

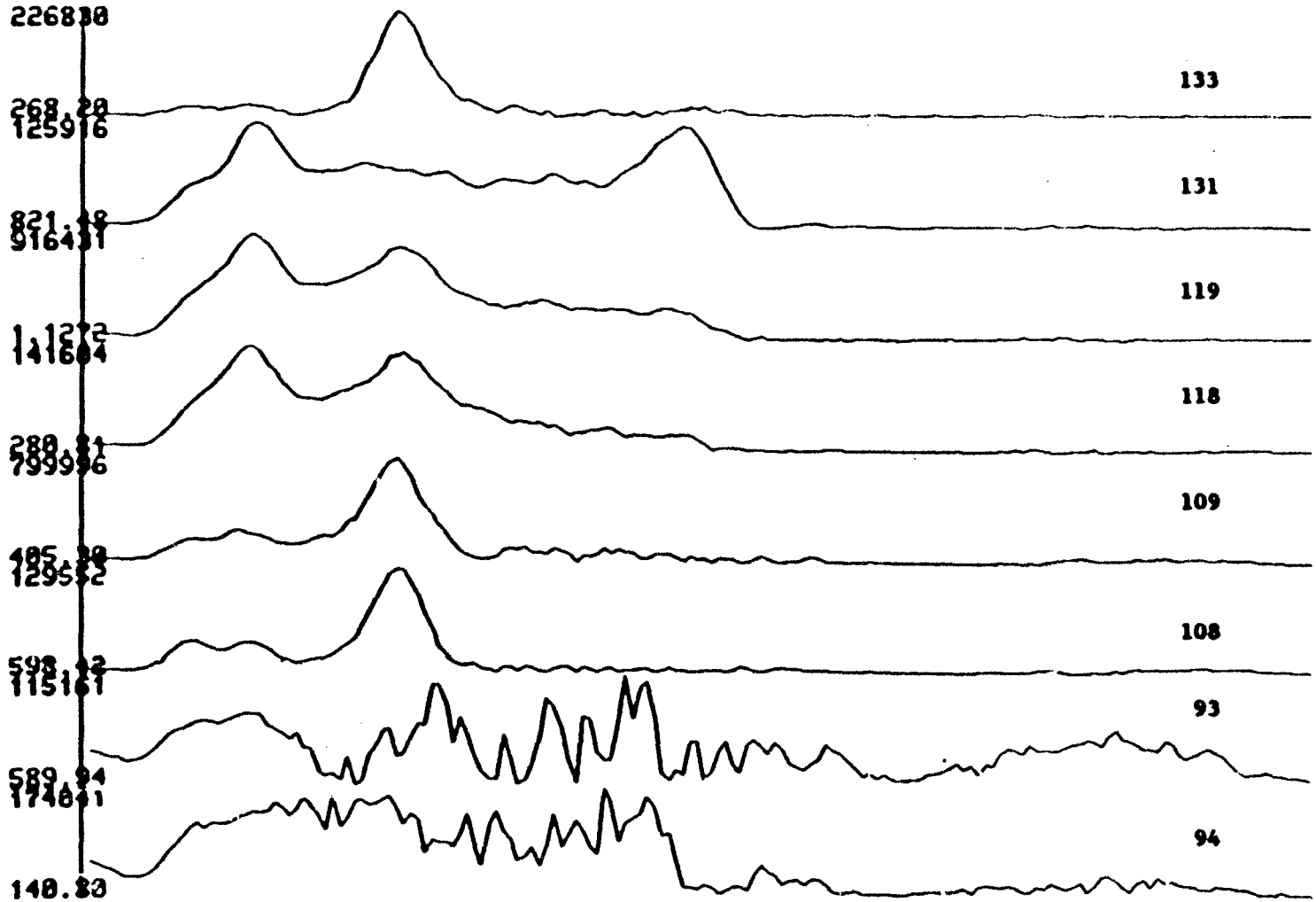

Figure 8. IMS Spectra of Phenol and HD After Application of an IFFT, the Digital Filter, and an FFT. Spectral range for the X-axis is 1.1-1.8 ratio of drift times, and the Y-axis units are arbitrary.

the HD peak. In more extreme cases where the ratio of the HD concentration to the phenol concentration is on the order of 1:5, less noticeable improvement can be seen (i.e., for this concentration no definitive statements may be made about the absence or presence of the HD peak). For concentrations less than 1:5, it appears that the HD signal does not exist in the data. It might be that no amount of signal processing will extract the HD features when phenol concentrations are greater than five times the HD concentrations.

This preliminary study indicates potential for enhancing the identification of IMS spectral features represented by small peaks adjacent to large peaks or as shoulders on peaks when the small peaks or shoulders are due to ionic species of interest. Future work in this area needs to be directed along the following lines:

- Using more sophisticated digital filters than those used in this study.

- Providing data smoothing routines for the filtered data to help determine the absence or presence of the HD peak.

- Creating a new software package for locating, identifying, and providing quantitative information about the agent peaks.

- Applying these data processing techniques to other IMS data.

APPENDIX

CONTENTS OF THE IMS/CAM DATABASE

CONTENTS OF THE IMS/CAM DATABASE

ENTRY NUMBER	EA NUMBER	NAME
1		PHENOL VAPOR
2		PHENOL VAPOR
3		PHENOL VAPOR
4		PHENOL VAPOR
5		PHENOL VAPOR
6		PHENOL VAPOR
7		PHENOL VAPOR
8		DECON KIT PACKET 1 (LOW)
9		DECON KIT PACKET 1 (LOW)
10		DECON KIT PACKET 1 (LOW)
11		DECON KIT PACKET 1 (LOW)
12		DECON KIT PACKET 1 (LOW)
13		DECON KIT PACKET 1 (MEDIUM)
14		DECON KIT PACKET 1 (MEDIUM)
15		DECON KIT PACKET 1 (MEDIUM)
16		DECON KIT PACKET 1 (MEDIUM)
17		DECON KIT PACKET 1 (MEDIUM)
18		DECON KIT PACKET 1 (MEDIUM)
19		DECON KIT PACKET 1 (MEDIUM)
20		DECON KIT PACKET 1 (MEDIUM)
21		DECON KIT PACKET 1 (HIGH)
22		DECON KIT PACKET 1 (HIGH)
23		DECON KIT PACKET 1 (HIGH)
24		DECON KIT PACKET 1 (HIGH)
25		DECON KIT PACKET 1 (HIGH)
26		DECON KIT PACKET 1 (HIGH)
27		DECON KIT PACKET 1 (HIGH)
28		DECON KIT PACKET 1 (HIGH)
29		DECON KIT PACKET 1 (HIGH)
30		DECON KIT PACKET 1 (HIGH)
31		DECON KIT PACKET 1 (HIGH)
32		BLANK - COVER OFF
33		BLANK - COVER OFF
34		BLANK - COVER OFF
35		BLANK - COVER OFF
36		BLANK - COVER OFF
37		PHENOL VAPOR
38		MUSTARD VAPOR AND PHENOL
39		PHENOL VAPOR
40		PHENOL VAPOR
41		PHENOL AND MUSTARD VAPOR
42		PHENOL VAPOR
43		PHENOL AND MUSTARD VAPOR
44		PHENOL AND MUSTARD VAPOR ?
45		PHENOL AND MUSTARD VAPOR

46	PHENOL AND MUSTARD VAPOR
47	PHENOL
48	PHENOL AND MUSTARD VAPOR
49	UNKNOWN
50	UNKNOWN
51	UNKNOWN
52	UNKNOWN
53	MUSTARD
54	MUSTARD
55	PHENOL
56	PHENOL
57	PHENOL AND MUSTARD VAPOR
58	PHENOL
59	PHENOL AND MUSTARD VAPOR
60	PHENOL
61	PHENOL AND MUSTARD VAPOR
62	PHENOL
63	PHENOL AND MUSTARD VAPOR
64	PHENOL
65	PHENOL AND MUSTARD VAPOR
66	MUSTARD VAPOR
67	MUSTARD VAPOR
68	MUSTARD VAPOR
69	MUSTARD VAPOR
70	MUSTARD VAPOR
71	MUSTARD AND PHENOL VAPOR
72	GENERATOR BLANK
73	GENERATOR BLANK WITH PHENOL
74	GENERATOR BLANK WITH PHENOL AND MUSTARD
75	BLANK GENERATOR WITH MUSTARD VAPOR
76	BLANK GENERATOR WITH MUSTARD VAPOR
77	MUSTARD VAPOR
78	MUSTARD AND PHENOL VAPOR
79	MUSTARD ???
80	PHENOL
81	PHENOL VAPOR
82	PHENOL VAPOR
83	PHENOL VAPOR
84	PHENOL AND HN3 VAPOR
85	PHENOL AND HN3 VAPOR
86	PHENOL AND HN3 VAPOR
87	PHENOL AND HN3 VAPOR
88	PHENOL AND HN3 VAPOR
89	PHENOL AND HN3 VAPOR
90	PHENOL AND HN3 VAPOR
91	PHENOL AND HN3 VAPOR ?
92	PHENOL
93	PHENOL VAPOR
94	PHENOL VAPOR
95	PHENOL VAPOR
96	PHENOL VAPOR
97	PHENOL AND HN3 VAPOR

98	PHENOL AND HN3 VAPOR
99	PHENOL AND HN3 VAPOR
100	PHENOL AND HN3 VAPOR
101	PHENOL AND HN3 VAPOR
102	PHENOL AND HN3 VAPOR
103	PHENOL AND HN3 VAPOR
104	PHENOL AND HN3 VAPOR
105	PHENOL AND HN3 VAPOR
106	PHENOL AND HN3 VAPOR
107	PHENOL AND HN3 VAPOR
108	PHENOL AND MUSTARD VAPOR
109	PHENOL AND MUSTARD VAPOR
110	PHENOL AND MUSTARD
111	PHENOL AND MUSTARD
112	MUSTARD VAPOR
113	MUSTARD VAPOR
114	MUSTARD VAPOR
115	MUSTARD VAPOR
116	MUSTARD VAPOR AND PHENOL
117	PHENOL AND MUSTARD VAPOR
118	PHENOL AND MUSTARD VAPOR
119	PHENOL AND MUSTARD VAPOR
120	PHENOL AND MUSTARD VAPOR
121	PHENOL AND MUSTARD VAPOR
122	PHENOL AND MUSTARD VAPOR
123	MUSTARD VAPOR
124	MUSTARD VAPOR AND PHENOL
125	PHENOL AND MUSTARD VAPOR
126	PHENOL AND MUSTARD VAPOR
127	PHENOL AND MUSTARD VAPOR
128	PHENOL AND MUSTARD VAPOR
129	PHENOL VAPOR
130	MUSTARD VAPOR AND PHENOL
131	PHENOL AND MUSTARD VAPOR
132	MUSTARD VAPOR
133	PHENOL AND MUSTARD VAPOR
134	HN3
135	HN3
136	HN3
137	HN3
138	HN3
139	HN3
140	HN3
141	HN3
142	HN3
143	HN3
144	HN3
145	HN3
146	HN3
147	PHENOL VAPOR
148	PHENOL AND HN3 VAPOR
149	PHENOL

150	PHENOL AND HN3 VAPOR
151	PHENOL
152	PHENOL AND HN3 VAPOR
153	PHENOL
154	PHENOL AND HN3 VAPOR
155	PHENOL
156	PHENOL AND HN3 VAPOR
157	HN3 VAPOR
158	PHENOL VAPOR
159	PHENOL VAPOR